$GABA_A$ Receptor-Mediated Cl^- Currents in Rat Thalamic Reticular and Relay Neurons

SHUANGLIN J. ZHANG, JOHN R. HUGUENARD, AND DAVID A. PRINCE
Department of Neurology and Neurological Sciences, Stanford University Medical Center, Stanford, California 94305

Zhang, Shuanglin J., John R. Huguenard, and David A. Prince. $GABA_A$ receptor-mediated Cl^- currents in rat thalamic reticular and relay neurons. *J. Neurophysiol.* 78: 2280–2286, 1997. Spontaneous and evoked inhibitory postsynaptic currents (sIPSCs and eIPSCs) and responses to exogenously applied γ-aminobutyric acid (GABA), mediated by GABA type A ($GABA_A$) receptors, were recorded in inhibitory neurons of nucleus reticularis thalami (nRt) and their target relay cells in ventrobasal (VB) nuclei by using patch clamp techniques in rat thalamic slices. The decay of sIPSCs in both nRt and VB neurons was best fitted with two exponential components. The decay time constants of sIPSCs in nRt neurons were much slower (τ_1 = 38 ms; τ_2 = 186 ms) than those previously reported in a variety of preparations and two to three times slower than those in VB neurons (τ_1 = 17 ms; τ_2 = 39 ms). $GABA_A$ receptor-mediated Cl^- currents directly evoked by local GABA application also had a much slower decay time constant in nRt (225 ms) than in VB neurons (115 ms). Slow decay of GABA responses enhances the efficacy of recurrent intranuclear inhibition in nRt. The results suggest a functional diversity of $GABA_A$ receptors that may relate to the known heterogeneity of $GABA_A$ receptor subunits in these two thalamic nuclei.

INTRODUCTION

Inhibitory circuits in the thalamus play a critical role in the generation of normal and pathophysiological thalamocortical rhythms (Steriade et al. 1993). γ-Aminobutyric acid-A ($GABA_A$) and/or type B ($GABA_B$) receptor-mediated inhibitory postsynaptic currents (IPSCs) in thalamic relay cells, which result from activation of nucleus reticularis (nRt) neurons, evoke rebound bursts that can reactivate nRt (Huguenard and Prince 1994a; von Krosigk et al. 1993). This recurrent circuitry is active during sleep spindles and perhaps in absence epilepsy. We demonstrated that a benzodiazepine (clonazepam) paradoxically decreases the GABAergic output of nRt (Huguenard and Prince 1994b), probably by enhancing the recurrent inhibitory circuitry within this nucleus. Clonazepam appeared to exert more powerful actions within nRt than in ventrobasal (VB) neurons, suggesting a heterogeneity of $GABA_A$ receptors, with those within nRt being more susceptible to benzodiazepine modulation than those on thalamic relay neurons (Zhang et al. 1994).

Regional differences in $GABA_A$ subunit composition are present within the thalamus, and the density of particular subunits does vary between nRt and relay nuclei (Fritschy and Mohler 1995; Gutiérrez et al. 1994; Wisden et al. 1992), implying that $GABA_A$ receptors with different functional properties might be present in these structures (Levitan et al. 1988; Verdoorn 1994; Verdoorn et al. 1990). Heterogeneity of GABA responses within a specific brain region was reported in cerebellar cortex where spontaneous inhibitory synaptic currents and GABA-evoked responses are longer lasting in granule cells than in Purkinje cells (Puia et al. 1994).

In the experiments reported here we examined the kinetic properties of $GABA_A$ receptor-mediated synaptic currents in visually identified nRt neurons and VB nuclear complex relay cells of thalamic slices. Results suggest that $GABA_A$ receptors in the two structures have different functional properties, especially with regard to their decay kinetics.

METHODS

Thalamic slices

Animal preparation was the same as described in detail in Huguenard and Prince (1994b) and Zhang and Jackson (1995). Briefly, 8- to 13-day old Sprague-Dawley rats were anesthetized with 50 mg/kg ip pentobarbital sodium, decapitated, and the brains rapidly removed and placed in chilled (4°C) artificial cerebral spinal fluid (aCSF) solution. Horizontal slices (300 μm) of thalamus were prepared with a vibratome (TPI, St. Louis, MO) and incubated for $\geq$1 h in gassed aCSF before being placed in a recording chamber. Thalamic neurons were viewed with an upright microscope (Zeiss, Thornwood, NY) equipped with differential interference contrast Nomarski optics and an electrically insulated ×40 water immersion objective with a working distance of 1.75 mm.

Solutions and drugs

The aCSF was composed of (in mM) 126 NaCl, 26 $NaHCO_3$, 2.5 KCl, 1.25 NaH_2PO_4, 2 $MgCl_2$, 2 $CaCl_2$, and 10 glucose and had a pH of 7.3 when equilibrated with the mixture of 95% O_2-5% CO_2. aCSF containing both 6-cyano-7-nitroquinoxaline-2,3-dione (CNQX; 20 μM) and 2-amino-5-phosphonovalerianic acid (APV; 200 μM) was used to block ionotropic glutamate receptor-mediated excitatory postsynaptic currents. 100 μM GABA and 20 μM bicuculline methiodide (BMI) solutions were made by adding GABA and BMI stock solutions to the CNQX/APV-containing aCSF. The slice was completely submerged in a total volume of 300 μl and continuously perfused at a rate of 4 ml/min. We estimated that 3–4 min were required to completely change solutions. The pipette solution contained (in mM) 135 CsCl, 5 QX-314, 2 $MgCl_2$, 10 ethylene glycol-bis(β-aminoethyl ether)-*N*,*N*,*N*′,*N*′-tetraacetic acid (EGTA), and 10 *N*-2-hydroxyethylpiperazine-*N*′-2-ethanesulfonic acid (HEPES). pH was adjusted to 7.2 with CsOH. GABA, BMI, and QX-314 were obtained from Sigma, CNQX and APV from RBI.

Electrophysiology

All voltage-clamp recordings were obtained at room temperature (22–24°C) with the continuous recording mode of an Axopatch-

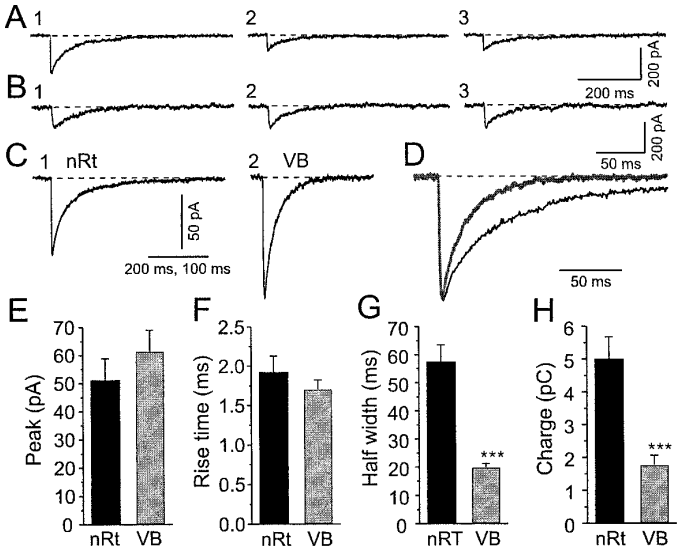

FIG. 1. Spontaneous inhibitory postsynaptic currents (sIPSCs) decay more slowly in nucleus reticularis thalami (nRt) than in ventrobasal (VB) neurons. *A* and *B*: single sIPSCs were recorded in nRt (A_{1-3}) and VB neurons (B_{1-3}) in the presence of 6-cyano-7-nitroquinoxaline-2,3-dione (CNQX; 20 μM) and amino-5-phosphonobutyric acid (AP5) (200 μM). Patch pipette contained the 135 mM CsCl internal solution. Note difference in time calibration in *A* and *B*. *C*: averages of 30 consecutive single isolated sIPSCs from nRt (C_1) and VB neurons (C_2). Superimposed on the averaged IPSCs are best-fitted double exponential curves. Note different time base in C_1 and C_2. Equation describing inhibitory postsynaptic potential (IPSP) decay was $-34.7*e^{-t/21.4} - 35.0*e^{-t/107}$ for nRt and $-26.6*e^{-t/7.4} - 87.3*e^{-t/25.8}$ for VB. *D*: averaged IPSCs in C_1 and C_2 are scaled to same amplitude and superimposed on same time base. *E*: average peak amplitudes of sIPSCs from 9 nRt and 15 VB neurons. Error bars represent mean ± SE. *F–H*: average rise time (*F*), half-width (*G*), and charge (*H*) from same neurons as in *E*. Charge transferred during sIPSCs was obtained by integrating IPSC trace over time (see text). ***$P \ll 0.001$.

200 amplifier (Axon Instruments, Foster City, CA) and the whole cell recording configuration of the patch-clamp technique (Hamill et al. 1981). Neurons were held at a holding potential of −60 mV. Electrodes were pulled from KG-33 borosilicate glass capillaries (1.5 mm OD, 1.0 mm ID; Garner Glass, Claremont, CA) that had resistances of 2–4 MΩ when filled with the internal solution. A bipolar tungsten electrode (impedance 0.1–1 MΩ; FHC, Brunswick, ME) placed within nRt was used to deliver electrical stimuli. GABA pulses were applied at 0.066 Hz via pressure ejection from a micropipette with a tip size of ~1.5 μm OD. Pressure and duration of GABA applications were adjusted so that the peak of the GABA-evoked current was comparable in amplitude to that of the standard electrically evoked IPSC.

Data analysis

Signals were filtered at 5 kHz (−3 dB, 8 pole, low-pass Bessel filter) and stored in digitized form (Neurocorder, Neurodata, NY) on VHS tape. CDR and SCAN software were used to collect continuous records and detect spontaneous events. Evoked IPSCs (eIPSCs) and GABA responses were recorded with pClamp 5.6 and analyzed with pClamp 6.1. Curve fittings were performed with Origin (MicroCal Software, Northampton, MA) and Clampfit 6.1.

RESULTS

Individual nRt and VB neurons within rat horizontal thalamic slices were visually identified by their location and some clearly discernable morphological characteristics, such as the shape of their cell bodies and distribution of proximal processes. The borders of nRt could be easily recognized in live slices, and neurons were selected that were well within its lateral and medial aspects, marked by the internal capsule and external medullary lamina, respectively. VB neurons were recorded from a region ≥100 μm medial to nRt. Much of the large dendritic tree of individual relay neurons could usually be observed in various focal planes above and below the soma. In a few cases, neurons of each type were filled with biocytin and subsequently processed immunohistochemically to confirm cell identity (Tseng et al. 1991). Care was taken to study cells 50–100 μm below the slice surface so that stable recordings could be obtained from apparently healthy neurons. The access resistance ranged from 5 to 17 MΩ (typically ~10 MΩ) and input resistance was ~400 MΩ in these cesium-loaded cells. Only those recordings with stable and low access resistance were included in the final analysis. Our results are derived from a total population of 45 nRt and 61 VB neurons.

Spontaneous IPSCs in nRt versus VB neurons

After ionotropic glutamate receptors were blocked with CNQX (20 μM) and APV (200 μM), spontaneous IPSCs (sIPSCs) were recorded in both nRt and VB neurons under whole cell voltage clamp at a holding potential of −60 mV. Typical sIPSCs, inward currents under these recording conditions (see METHODS), are shown for nRt and VB neurons in the *top panels* of Fig. 1, A_{1-3} and B_{1-3}, respectively). Averages of 30 consecutive sIPSCs recorded from single nRt and VB neurons are shown in Fig. 1, C_1 and C_2, respectively. Responses scaled to the same amplitude are shown in Fig. 1*D* to illustrate differences in time course.

As previously reported in other preparations (Edwards et al. 1990; Puia et al. 1994), spontaneous GABA$_A$ receptor-mediated IPSCs were highly variable in amplitude, ranging from 20 to 200 pA. The peak amplitudes of the averaged sIPSCs were slightly lower in nRt (51.2 ± 7.7 pA, mean ± SE, $n = 9$) than in VB neurons (61.4 ± 7.6 pA, $n = 15$; Fig. 1*E*), but this difference was not significant ($P = 0.4$). Bath perfusion with GABA$_A$ receptor antagonist BMI (20 μM) completely abolished sIPSCs in both nRt and VB neurons (Fig. 2). With an expected reversal potential of 0 mV, the peak IPSC current amplitudes in symmetric Cl$^-$ corre-

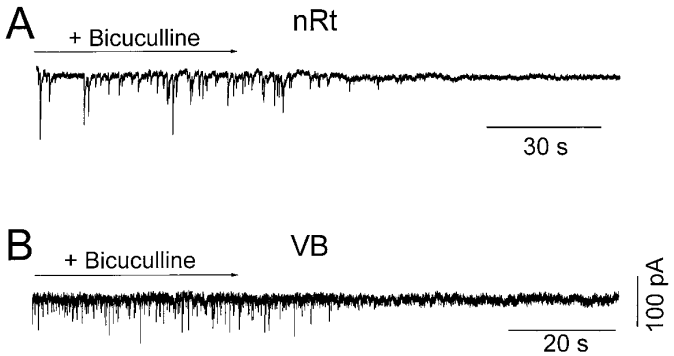

FIG. 2. sIPSCs in VB and nRt are γ-aminobutyric acid-A (GABA$_A$) receptor-mediated. sIPSCs in nRt (*A*) and VB neuron (*B*) were blocked completely by bicuculline methiodide (BMI; 20 μM). Access resistance before and after addition of BMI was 14 MΩ in *A* and 15 MΩ in *B*.

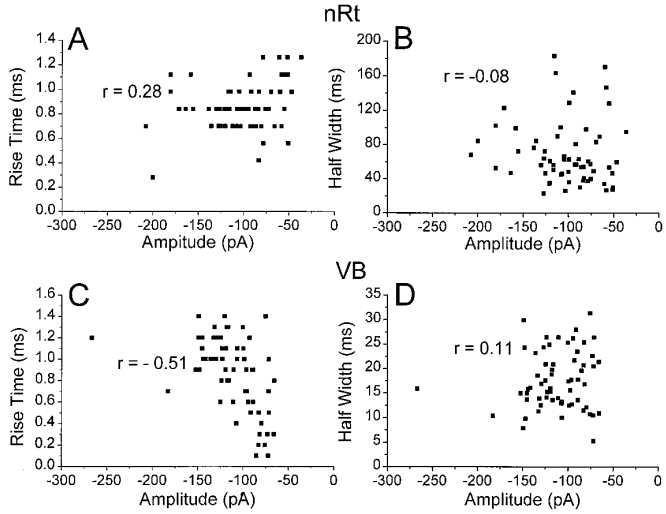

FIG. 3. Plots of rise time (*A*, *C*) and half-width (*B*, *D*) vs. amplitude of sIPSCs in nRt (*A*–*B*) and VB neuron (*C*–*D*). Linear regressions fittings generated the correlation coefficients (*R*) indicated. Each point was derived from single sIPSC. Correlations were low in each case suggesting that dendritic filtering played little role in shaping IPSCs. There are no differences in these parameters between nRt and VB neurons, which suggests that the differences in decay time constants are not due to the geometric differences between these 2 types of neurons.

sponded to conductances of ~0.85 nS in nRt and 1.0 nS in VB neurons. These values are similar to those in other types of neurons such as dentate gyrus (Edwards et al. 1990; Otis and Mody 1992) and cerebellar granule cells (Puia et al. 1994).

The rise times of sIPSCs, measured as the time between points at 10 and 90% of peak current amplitude, were not significantly different for nRt neurons (2.1 ± 0.2 ms, n = 9) versus VB relay cells (1.7 ± 0.1 ms, n = 15, P = 0.1; Fig. 1*F*). The plots of Fig. 3, *A* and *C*, show that there was little correlation between the distribution of sIPSC amplitude versus rise time in nRt and VB, and similarly, half-width was almost independent of amplitude ($R \approx 0.1$) in the two groups of neurons (Fig. 3, *B* and *D*). The lack of such correlations has been used to argue against a strong influence of electrotonic filtering on the shape of recorded sIPSCs (Silver et al. 1992). However, it was also suggested that a linear relationship between rise time and amplitude would not necessarily be expected in a complex dendritic arbor (Major et al. 1994; Ulrich and Luscher 1993). Furthermore, recent evidence from dentate granule cells suggests that only proximal (i.e., perisomatic) IPSCs are obtained with whole cell somatic recordings (Soltesz et al. 1995). Assuming similar IPSC activation kinetics, the equivalent rise times in VB and nRt neurons suggest that events at similar electrotonic distances were recorded in each cell type.

Because rise times were similar in both cell types, differences in half-width (i.e., the width of the IPSC at half-maximal amplitude) should reveal differences in decay kinetics. This simplified measure makes no assumptions regarding the underlying mechanism that terminates the $GABA_A$ responses and therefore provides an unbiased estimate of spontaneous inhibitory postsynaptic potential (sIPSP) duration. The average half-width was approximately three times longer in nRt (57.5 ± 6.0 ms, n = 9) than in VB (19.9 ± 1.3 ms, n = 15), a difference that was highly significant ($P = 1 \times 10^{-7}$; Fig. 1*G*). Although sIPSC decay kinetics could not be well fitted with a single exponential in either VB or nRt neurons, double exponential curves closely approximated the data (Fig. 1, C_1 and C_2). The two time constants of decay (τ_1, fast; τ_2, slow) were both larger in nRt (τ_1, 37.5 ± 3.8 ms; τ_2, 186.1 ± 18.3 ms) than VB neurons (τ_1, 16.7 ± 1.8 ms; τ_2, 39.0 ± 2.9 ms; Table 1).

Inhibitory efficacy of sIPSCs was estimated by calculating the total Cl^- charge movement. This measure takes into account both amplitude and time course of the inhibitory events and was obtained by integrating the averaged sIPSC from each cell over time. As shown in Fig. 1*H*, the efficacy of sIPSCs was much greater in nRt neurons (5.0 ± 0.7 pC, n = 9) than in VB cells (1.8 ± 0.3 pC, n = 15, $P = 4 \times 10^{-5}$). Furthermore, analysis of the slowly and rapidly decaying sIPSC components demonstrated that most of the charge (~4 pC) arose from the slow component in nRt cells, compared with about one-half (~1 pC) in VB cells (see values for C_1 and C_2 in nRt and VB given in Table 1).

Electrically evoked IPSCs in nRt and VB neurons

We next compared the properties of evoked IPSPs in the two nuclei. Immediately after obtaining a whole cell recording, a few test stimuli were delivered via a bipolar tungsten electrode placed within nRt to check the synaptic responsiveness of the neuron. Once responses were clearly seen, monosynaptic eIPSCs were isolated by switching the perfusion solution from normal aCSF to one containing CNQX and APV. After ~4 min, when excitatory ionotropic synaptic responses were blocked, a series of test stimuli of increasing intensity (10–250 μA and 10–200 μs) was applied to obtain the threshold for evoking monosynaptic IPSCs. Stimuli were adjusted to be 1.5 times threshold for eliciting a detectable monosynaptic IPSC in each neuron (100–300 μA; 60–300 μs). The average peak eIPSC amplitude in nRt cells (130.8 ± 25.0 pA, n = 10) was significantly smaller than that in VB neurons (465.7 ± 100.6 pA, n = 11, P = 0.006; Fig. 5*D*).

The reversal potential for eIPSCs was 3.2 ± 1.4 mV (n =

TABLE 1. *Exponential decay properties of sIPSCs*

Parameters	nRt Neurons	VB Neurons	*P*-Value
τ_1 (ms)	37.5 ± 3.8	16.7 ± 1.8	≪0.001
A_1 (pA)	30.5 ± 6.5	40.2 ± 5.7	NS
C_1 (pC)	1.1 ± 0.2	0.7 ± 0.1	<0.05
τ_2 (ms)	186.1 ± 18.3	39.0 ± 2.9	≪0.001
A_2 (pA)	23.8 ± 3.9	29.4 ± 5.3	NS
C_2 (pC)	4.2 ± 0.7	1.1 ± 0.2	≪0.001

Values are means ± SE; number of nRt neurons was 9 and VB neurons was 15. Double exponential functions were fitted to averaged spontaneous inhibitory postsynaptic currents (sIPSCs). Each average was composed of a minimum of 30 individual events. τ_1 and τ_2 are time constants for the fast and slow decay phases, respectively, while A_1, A_2 and C_1, C_2 are the zero-time amplitudes and charge movements for each decay phase, respectively. Values of A_1, A_2, C_1, and C_2 represent contributions of fast and slow decay phases to total decay. Both fast and slow time constants were significantly different. nRt, nucleus reticularis thalami; VB, ventrobasal; NS, not significant.

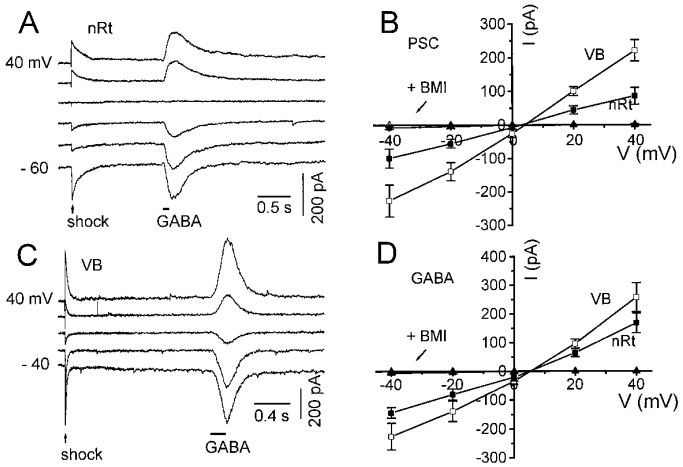

FIG. 4. Evoked IPSCs (eIPSCs) and GABA responses are GABA$_A$ receptor-mediated. *A* and *C*: electrically evoked IPSCs (⁄) and responses to pressure pulses of GABA (100 μM; ■) at a range of membrane potentials between −60 and +40 mV (20 mV steps) in nRt (*A*) and VB neuron (*C*). Responses of both types reversed near 0 mV in both neurons. Note different time calibrations in *A* and *C*. *B* and *D*: *I-V* curves for IPSCs (*B*) and GABA-evoked responses (*D*) from nRt (■) and VB neurons (□) reversed at ~0 mV. Addition of 20 μM BMI in the perfusion solution completely blocked IPSCs in VB (*B*, △) and nRt (*B*, ▲) as well as GABA responses (*D*, △ and ▲). Recordings obtained with symmetrical [Cl^-]; calculated E_{Cl} = 0 mV. PSC, postsynaptic current.

TABLE 2. *Decay properties of evoked IPSCs*

Parameters	nRT Neurons	VB Neurons	*P*-Value
τ_1 (ms)	42.5 ± 6.1	23.0 ± 3.4	<0.05
A_1 (pA)	54.0 ± 12.4	320.0 ± 77.1	<0.01
C_1 (pC)	2.6 ± 0.9	6.1 ± 1.4	NS
τ_2 (ms)	177.6 ± 16.4	68.3 ± 6.7	≪0.001
A_2 (pA)	72.9 ± 18.4	126.8 ± 29.2	NS
C_2 (pC)	12.4 ± 3.0	7.4 ± 1.2	NS

Values are means ± SE; number of nRt neurons was 10 and VB neurons was 11. Double exponential functions were fitted to averaged evoked IPSs (eIPSCs). Each average was composed of a minimum of 20 individual events. τ_1, τ_2, A_1, A_2, C_1, and C_2 are parameters describing the decay process and are equivalent to those used for sIPSCs (see Table 1). Both slow and fast time constants, τ_1 and τ_2 were significantly longer in nRt compared to VB neurons. Amplitude of the fast component was larger in VB neurons, whereas proportion of slow decay was larger in nRt neurons. NS, not significant. See Table 1 for other abbreviations.

5) in nRt and 1.8 ± 1.1 mV (n = 5) in VB (Fig. 4, *A*–*C*), values near the expected reversal potential for Cl^- ions (0.5 mV; $[Cl]_i/[Cl]_o$ = 139/136.5). The conductance of the IPSCs evoked by 1.5 times threshold stimuli, obtained from linear regression of the *I-V* curves, was 2.4 ± 0.6 nS in nRt compared with 5.7 ± 0.9 nS in VB (Fig. 4*B*). Evoked IPSCs were completely abolished by the specific GABA$_A$ antagonist BMI (20 μM; Fig. 4*B*, ▲).

As with sIPSCs, the half-width of eIPSCs was significantly longer in nRt (72.0 ± 6.0 ms, n = 10) than in VB neurons (27.0 ± 3.6 ms, n = 11, $P = 3 \times 10^{-6}$; Fig. 5, *C* and *E*). In each case the decay phase of eIPSCs was best described by the sum of two exponentials (Fig. 5, *A* and *B*), with τ_1 = 42.5 ± 6.1 ms and τ_2 = 177.6 ± 16.4 ms in nRt neurons (n = 10) and τ_1 = 23.0 ± 3.4 ms and τ_2 = 68.3 ± 6.7 ms in VB neurons (n = 11; Table 2). Both fast and slow components were significantly different between the two cell groups, with *P*-values of 0.01 and 4.0×10^{-6}, respectively. The slow component was always present in both cell types, but more prominent in nRt neurons. The average contributions of both fast and slow components to the eIPSC peak current are shown in Table 2 by the values of A_1 and A_2, respectively.

eIPSCs had a larger amplitude in VB neurons (Fig. 5*D*), but were longer lasting in nRt cells (Fig. 5*E*; Table 2). We compared the efficacy of eIPSCs in the two structures by measuring the average charge of events evoked by stimuli that were 1.5 times threshold. In nRt neurons the average charge during an eIPSC was 18.0 ± 4.0 pC (n = 10), compared with 16.3 ± 2.8 pC in VB neurons (n = 11; Fig. 5*F*), values that were not significantly different (P = 0.7). As with spontaneous IPSCs, most of the charge transferred during evoked events was carried by the slowly decaying component in nRt cells, but in VB neurons similar contributions were made by the fast and slow components (Table 2). The average 1.5 times threshold stimulus intensity tended to be higher for nRt [23.2 ± 3.8 nC (ms·μA), n = 10] than VB (14.9 ± 2.0 nC, n = 11), but these values were not significantly different (P = 0.06).

GABA-evoked responses in nRt and VB neurons

To further assess the properties of IPSCs in VB and nRt neurons we tested responses to pressure pulses of GABA (100 μM; 7–27 kPa and 10–200 ms) delivered onto the visualized recorded neuron via a micropipette. The peak amplitude of the GABA response, which varied depending on the pressure and duration of pressure ejections and the tip size of ejection pipettes, was adjusted to be approximately the same as that of an IPSC evoked by 1.5 times threshold

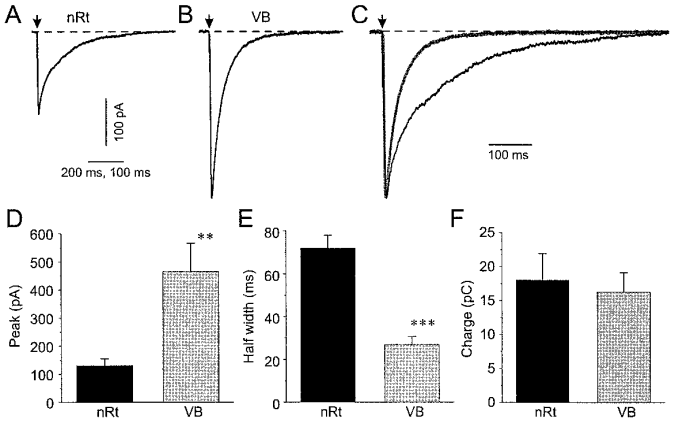

FIG. 5. Electrically evoked IPSCs recorded from thalamic neurons. *A* and *B*: averages of 20 consecutive single isolated IPSCs evoked in nRt (*A*) and VB neuron (*B*) by 1.5 times threshold stimuli (↓). Double exponential fits are superimposed on actual averaged traces. Time calibration bar: 200 (*A*) and 100 ms (*B*). Fitted curves are described by $-45.3*e^{-t/15.5} - 131*e^{-t/158}$ for the nRt and $-222*e^{-t/22.7} - 136*e^{-t/61.1}$ for the VB neuron. *C*: averaged traces from nRt (from *A*, dark line) and VB (from *B*, gray line) neurons are scaled to the same amplitude and superimposed on same time base for direct comparison. *D*–*F*: graphs of average peak eIPSC amplitude (*D*), eIPSC half-width (*E*), and eIPSC total charge (*F*) for nRt vs. VB neurons. **P < 0.01; ***P ≪ 0.001.

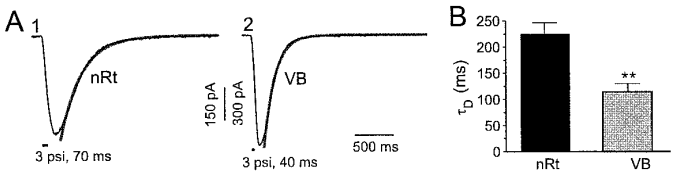

FIG. 6. GABA-evoked $GABA_A$ receptor-mediated responses in nRt and VB neurons. *A*: averaged traces of 20 responses evoked by 100 μM GABA pressure pulses in nRt (A_1) and VB (A_2) neuron. Single exponential function was fitted to decay phase of averaged traces and is superimposed. Fitted curves were described by $-433*e^{-t/268}$ for nRt and $-917*e^{-t/141}$ for VB. *B*: decay time constants for GABA responses from nRt and VB neurons were significantly different (see text). $^{**}P < 0.01$.

stimuli (e.g., see Fig. 4, *A* and *C*). Although the GABA responses varied in amplitude from cell to cell, the decay rate of the response was relatively constant among neurons within a given nucleus. These GABA-evoked currents were $GABA_A$ receptor-mediated, because they reversed at the same potential as the electrically evoked IPSCs (Fig. 4, *A*, *C*, and *D*) and were also blocked by 20 μM bicuculline (Fig. 4*D*). The reversal potentials were 0.9 ± 2.2 mV (n = 4) in nRt and 1.0 ± 0.8 mV (n = 4) in VB neurons. The decay phases of GABA responses were best fitted with single exponential functions (Fig. 6, A_1 and A_2) and, as was the case for sIPSCs and eIPSCs, the decay time constants were significantly longer in nRt (224.8 ± 22.2 ms, n = 7) versus VB neurons (115.0 ± 15.4 ms, n = 8, P = 0.001; Fig. 6*B*).

DISCUSSION

The principal finding in these experiments is a heterogeneity of functional inhibition in rat somatosensory thalamus. Most inhibition within this structure originates from neurons of the nucleus reticularis thalami (Yen et al. 1985), although an extrinsic inhibitory pathway has been described (Keller et al. 1992). Thus in these experiments spontaneous and evoked synaptic currents primarily reflect $GABA_A$ receptor-mediated postsynaptic events triggered by activity in nRt axons and terminals. It is interesting to note that similar presynaptic nRt activity results in very different responses that depend on the postsynaptic target neuron. IPSCs in relay neurons that arise from afferent nRt fibers are relatively short-lived (half-width ~20 ms), whereas IPSCs in nRt neurons that result from activity in recurrent local collaterals (Cox et al. 1996; Spreafico et al. 1988; Yen et al. 1985) are prolonged by comparison (~60 ms). In addition, the responses elicited by pressure-ejection of GABA are almost two times longer lasting in nRt (decay time constant ~225 ms) than in VB (~115 ms) neurons. The decay of IPSCs and GABA-elicited responses in nRt cells are much slower than those reported for most other types of neurons (Edwards et al. 1990; Puia et al. 1994; Zhang and Jackson 1993), with the exception of hippocampal inhibitory cells in culture (Jones and Westbrook 1995). The decay phase of IPSCs in both nuclei is composed of two exponentials, which likely reflect the intrinsic properties of the $GABA_A$ receptor channels, as was suggested in cerebellar granule neurons (Puia et al. 1994).

The differences between nRt and VB cannot be explained easily by technical artifacts such as space-clamp problems, because IPSCs in both structures had reversal potentials close to those expected given the recording conditions. Also, pipettes with similar resistances were used, and comparable seal and access resistances were obtained in recordings from both types of neuron. The similar rise times of $GABA_A$ receptor-mediated responses in nRt and VB (Figs. 1, *D* and *F*) indicate that the differences in the decay of either IPSCs or direct GABA-elicited responses in neurons of these structures were not due to differences in electrotonic structure. The possibility that a $GABA_B$-mediated component was present in nRt neurons is eliminated by the use of Cs^+ and QX-314 in the patch pipettes (Nathan et al. 1990), the single reversal potential of the postsynaptic currents at $\sim E_{Cl}$ (Fig. 4, *A*–*C*), and the complete blockade in BMI.

These differences in IPSC time course are likely due to differences in $GABA_A$ receptors in the two populations of cells. This conclusion is indirectly supported by the finding that the responses evoked by GABA applications displayed congruent differences in decay kinetics (Fig. 6). Further support for $GABA_A$ receptor heterogeneity within these two thalamic nuclei was provided by results of in situ hybridization and immunocytochemical localization studies indicating that nRt and the VB nuclear complex possess different distributions of $GABA_A$ receptor subunit mRNAs and proteins, as well as the finding that GABA responses in nRt and VB cells are differentially modulated by midazolam (Zhang et al. 1994, 1996) and zinc (Kang et al. 1996).

What might lead to long-lasting inhibitory responses in nRt cells? The decay of sIPSCs and eIPSCs at GABAergic synapses is dependent on a complex series of events, including neurotransmitter diffusion and reuptake, receptor desensitization, and the kinetic properties of the postsynaptic channels themselves (Roepstorff and Lambert 1994). Inhibition of GABA uptake does not alter the time course of inhibitory synaptic responses, at least in hippocampal slices (Isaacson et al. 1993), making it unlikely that slowed GABA uptake prolongs IPSPs at intra-nRt synapses. Also, it has been proposed that diffusion is a very rapid process in the synaptic cleft (Busch and Sakmann 1990; Clements 1996; Korn and Faber 1987; Wathey et al. 1979), suggesting that the differences in IPSC time course at nRt versus VB synapses are not due to diffusional differences. The finding that a benzodiazepine compound alters the decay time constant of the GABA responses (Zhang et al. 1994) is consistent with the idea that the kinetics of the response are largely determined by the properties of the GABA receptors themselves and not to other factors such as reuptake, diffusion, etc. Thus the most likely explanation for these findings is a heterogeneity in the properties of GABA receptor Cl^- channels. Channel reopenings during bursts (Bormann and Clapham 1985; De Koninck and Mody 1994; Weiss and Magleby 1989; Zhang and Jackson 1995) can lead to an extended total response (Zhang and Jackson 1994), so one possibility is that burst duration is longer for $GABA_A$ channels in nRt neurons than for those in VB cells. Single channel data showing longer open times in nRt than VB suggest that this is the case (Kang et al. 1996). It is also possible that GABA receptor desensitization (Puia et al. 1994) may be less prominent in nRt neurons and/or that reopenings from the desensitized state (Jones and Westbrook 1995) are more likely in these cells.

Suggested basis of IPSC difference: heterogeneity of $GABA_A$ receptors

The suggestion that there are fundamental differences in $GABA_A$ receptors (channels) in nRt and VB neurons gains support from anatomic studies of $GABA_A$ receptors in the thalamus and also from pharmacological and single channel studies. For example, immunocytochemical experiments have shown that $\alpha 1$, $\beta 2$, and $\beta 3$ subunit proteins are abundant in VB but absent in nRt, whereas the $\alpha 3$ subunit is prominent in nRt and absent in VB (Fritschy and Mohler 1995). In situ hybridization experiments also indicate a heterogeneity of subunits in different nuclei so that $\alpha 1$, $\alpha 4$, and δ mRNAs are abundant in VB but only weakly present in nRt (Wisden et al. 1992). The precise composition of native $GABA_A$ receptors is not known in thalamus or other CNS structures, nor has a detailed correlation between subunit composition and the kinetic properties of $GABA_A$ receptor channels been possible (Macdonald and Olsen 1994). However, data from studies of recombinant receptors make it likely that the structural differences detected to date will be reflected in different receptor properties (Dominguez-Perrot et al. 1995; Gingrich et al. 1995; Verdoorn 1994; Verdoorn et al. 1990). For example, $\alpha 3$ subunits when coexpressed with $\beta 2$ and $\gamma 2$ in HEK293 cells give rise to slower activation, deactivation, and desensitization than comparable receptors containing the $\alpha 1$ subunit (Gingrich et al. 1995; Verdoorn 1994). Differences in sensitivity of IPSCs in VB versus nRt to benzodiazepines (Zhang et al. 1996) and zinc (Kang et al. 1996), as well as different kinetics of single channels in the two structures (Kang et al. 1996) support this assumption. Single channel studies of native receptors whose subunit composition is known will be required to determine the bases for the physiological differences in IPSCs in neurons of VB and nRt described here.

Functional implications

Recurrent inhibitory circuitry within nRt is a powerful regulator of synchronized network activity. Focal application of BMI within nRt increases the inhibitory output from nRt onto VB (Huguenard and Prince 1994a) and bath BMI application enhances the extent and duration of 3-Hz network oscillations in thalamic slices (Huguenard and Prince 1994b; von Krosigk et al. 1993). In addition, BMI induces a very large increase in the duration of calcium-dependent bursts during synchronized network activity in perigeniculate (PGN) neurons (Bal et al. 1995), which in ferret dorsal lateral geniculate are analogous to nRt cells. This latter finding suggests that recurrent inhibition in nRt/PGN can hyperpolarize neurons in these structures and/or shunt the calcium-dependent burst-firing response that is induced by excitatory synaptic currents during network activity. The long-lasting nature of the intra-nRt IPSP described here may then enhance shunting and lead to early termination of the bursts. On the other hand, if E_{Cl} is sufficiently negative, IPSPs in nRt cells may lead to calcium channel deinactivation and generation of rebound burst discharge.

Because of differences in slice connectivity and divergence and convergence of afferents, it is difficult to normalize electrically evoked responses across different nuclei. Nevertheless, the peak amplitude of IPSCs evoked by standard stimuli (1.5 times threshold) was approximately four times larger in VB than nRt neurons. Because the range of stimulus intensities for evoking IPSCs was similar for each cell type (8–50 nC), it is likely that similar numbers of nRt cells were activated in each case. Both spontaneous (Fig. 1, *D* and *E*) and miniature (Ulrich and Huguenard 1996) IPSCs have comparable sizes in the two nuclei. Because miniature events presumably reflect quantal release, this difference in evoked response amplitude suggests that the total number of functional synapses or release sites is larger in VB cells than in nRt neurons. Support for this conclusion is also provided by the finding that frequency of miniature IPSCs was approximately three times higher in VB than in nRt neurons (Ulrich and Huguenard 1996). This inference from electrophysiological data is consistent with anatomic observations. The axonal projection patterns of nRt neurons (Cox et al. 1996; Scheibel and Scheibel 1966; Yen et al. 1985) suggest widespread connections with large numbers of putative release sites in relay nuclei but few axon collaterals within nRt. In spite of this, the net effective inhibition, as measured by total Cl^- flux during the evoked IPSC, was approximately equal in nRt and VB cells (Fig. 5*F*), indicating that the long duration of the intra-nRt IPSC compensates for the lower level of connectivity to produce equivalent inhibitory output.

One likely consequence of long-lasting inhibitory postsynaptic potentials in nRt neurons would be a limitation in the frequency range of repetitive network activity. The slow time constant of evoked IPSC decay was 180 ms (Table 2). If we assume a temperature coefficient of 2.0 (Otis and Mody 1992), at 37°C slow decay would be 67% complete in ~70 ms, thus restricting network repetitive activity to frequencies less than ~14 Hz. The contribution of intra-nRt connectivity to rhythmic activity during sleep spindles remains controversial (McCormick and Bal 1994; Steriade 1995), but the prolonged IPSC decay demonstrated here is consistent with theoretical studies of spindlelike synchrony in an interconnected network of inhibitory cells (Destexhe et al. 1993; Golomb et al. 1994).

CDR and SCAN software was graciously provided by Dr. J. Dempster.

This work was supported by National Institutes of Health Grant NS-06477 and training grant HL-07740 and Pimley Research and Training funds. S. J. Zhang was supported by Dr. Phyllis Gardner during completion of data analysis and manuscript preparation.

Present address of S. J. Zhang: Dept. of Molecular Pharmacology, Stanford University School of Medicine, Stanford, CA, 94305.

Address for reprint requests: J. R. Huguenard, Dept. of Neurology and Neurological Sciences, Room M016, Stanford University Medical Center, Stanford, CA 94305-5300.

Received 28 January 1997; accepted in final form 8 July 1997.

REFERENCES

BAL, T., VON KROSIGK, M., AND MCCORMICK, D. A. Role of ferret perigeniculate nucleus in the generation of synchronized oscillations in vitro. *J. Physiol. (Lond.)* 483: 665–685, 1995.

BORMANN, J. AND CLAPHAM, D. E. γ-Aminobutyric acid receptor channels in adrenal chromaffin cells: a patch-clamp study. *Proc. Natl. Acad. Sci. USA* 82: 2168–2172, 1985.

BUSCH, C. AND SAKMANN, B. Synaptic transmission in hippocampal neurons: numerical reconstruction of quantal IPSCs. *Cold Spring Harb. Symp. Quant. Biol.* 55: 69–80, 1990.

CLEMENTS, J. D. Transmitter timecourse in the synaptic cleft: its role in central synaptic function. *Trends Neurosci.* 19: 163–171, 1996.

COX, C. L., HUGUENARD, J. R., AND PRINCE, D. A. Heterogeneous axonal arborizations of rat thalamic reticular neurons in the ventrobasal nucleus. *J. Comp. Neurol.* 366: 416–430, 1996.

DE KONINCK, Y. AND MODY, I. Noise analysis of miniature IPSCs in adult rat brain slices: properties and modulation of synaptic $GABA_A$ receptor channels. *J. Neurophysiol.* 71: 1318–1335, 1994.

DESTEXHE, A., MCCORMICK, D. A., AND SEJNOWSKI, T. J. A model for 8–10 Hz spindling in interconnected thalamic relay and reticularis neurons. *Biophys. J.* 65: 2473–2477, 1993.

DOMINGUEZ-PERROT, C., FELTZ, P., AND POULTER, M. O. Recombinant $GABA_A$ receptor desensitization: the role of the gamma 2 subunit and its physiological significance. *J. Physiol. (Lond.)* 497: 145–159, 1996.

EDWARDS, F. A., KONNERTH, A., AND SAKMANN, B. Quantal analysis of inhibitory synaptic transmission in the dentate gyrus of rat hippocampal slices: a patch-clamp study. *J. Physiol. (Lond.)* 430: 213–249, 1990.

FRITSCHY, J. M. AND MOHLER, H. $GABA_A$-receptor heterogeneity in the adult rat brain: differential regional and cellular distribution of seven major subunits. *J. Comp. Neurol.* 359: 154–194, 1995.

GINGRICH, K. J., ROBERTS, W. A., AND KASS, R. S. Dependence of the $GABA_A$ receptor gating kinetics on the α-subunit isoform: implications for structure-function relations and synaptic transmission. *J. Physiol. (Lond.)* 489: 529–543, 1995.

GOLOMB, D., WANG, X. J., AND RINZEL, J. Synchronization properties of spindle oscillations in a thalamic reticular nucleus model. *J. Neurophysiol.* 72: 1109–1126, 1994.

GUTIÉRREZ, A., KHAN, Z. U., AND DE BLAS, A. L. Immunocytochemical localization of γ2 short and γ2 long subunits of the $GABA_A$ receptor in the rat brain. *J. Neurosci.* 14: 7168–7179, 1994.

HAMILL, O. P., MARTY, A., NEHER, E., SAKMANN, B., AND SIGWORTH, F. J. Improved patch clamp techniques for high-resolution current recordings from cells and cell free patches. *Pflügers Arch.* 391: 85–100, 1981.

HUGUENARD, J. R. AND PRINCE, D. A. Clonazepam suppresses $GABA_B$-mediated inhibition in thalamic relay neurons through effects in nucleus reticularis. *J. Neurophysiol.* 71: 2576–2581, 1994a.

HUGUENARD, J. R. AND PRINCE, D. A. Intrathalamic rhythmicity studied in vitro: nominal T-current modulation causes robust antioscillatory effects. *J. Neurosci.* 14: 5485–5502, 1994b.

ISAACSON, J. S., SOLIS, J. M., AND NICOLL, R. A. Local and diffuse synaptic actions of GABA in the hippocampus. *Neuron* 10: 165–175, 1993.

JONES, M. V. AND WESTBROOK, G. L. Desensitized states prolong $GABA_A$ channel responses to brief agonist pulses. *Neuron* 15: 181–191, 1995.

KANG, J., HUGUENARD, J. R., AND PRINCE, D. A. Single channel properties of neuronal $GABA_A$ receptors in rat nucleus reticularis thalami (nRt) and ventrobasal relay complex (VB). *Soc. Neurosci. Abstr.* 22: 97, 1996.

KELLER, A., ARISSIAN, K., AND ASANUMA, H. Synaptic proliferation in the motor cortex of adult cats after long-term thalamic stimulation. *J. Neurophysiol.* 68: 295–308, 1992.

KORN, H. AND FABER, D. Regulation and significance of probabilistic release mechanisms at central synapses. In: *Synaptic Function*, edited by G. Edelman, E. Gall, and W. M. Cowan. New York: Wiley, 1987, p. 57–108.

LEVITAN, E. S., BLAIR, L. A., DIONNE, V. E., AND BARNARD, E. A. Biophysical and pharmacological properties of cloned $GABA_A$ receptor subunits expressed in *Xenopus* oocytes. *Neuron* 1: 773–781, 1988.

MACDONALD, R. L. AND OLSEN, R. W. $GABA_A$ receptor channels. *Annu. Rev. Neurosci.* 17: 569–602, 1994.

MAJOR, G., LARKMAN, A. U., JONAS P., SAKMANN, B., AND JACK, J. J. Detailed passive cable models of whole-cell recorded CA3 pyramidal neurons in rat hippocampal slices. *J. Neurosci.* 14: 4613–4638, 1994.

MCCORMICK, D. A. AND BAL, T. Sensory gating mechanisms of the thalamus. *Curr. Opin. Neurobiol.* 4: 550–556, 1994.

NATHAN, T., JENSEN, M. S., AND LAMBERT, J. D. The slow inhibitory postsynaptic potential in rat hippocampal CA1 neurones is blocked by intracellular injection of QX-314. *Neurosci. Lett.* 110: 309–313, 1990.

OTIS, T. S. AND MODY, I. Modulation of decay kinetics and frequency of $GABA_A$ receptor-mediated spontaneous inhibitory postsynaptic currents in hippocampal neurons. *Neuroscience* 49: 13–32, 1992.

PUIA, G., COSTA, E., AND VICINI, S. Functional diversity of GABA-activated Cl^- currents in Purkinje versus granule neurons in rat cerebellar slices. *Neuron* 12: 117–126, 1994.

ROEPSTORFF, A. AND LAMBERT, J.D.C. Factors contributing to the decay of the stimulus-evoked IPSC in rat hippocampal CA1 neurons. *J. Neurophysiol.* 72: 2911–2926, 1994.

SCHEIBEL, M. E. AND SCHEIBEL, A. B. The organization of the nucleus reticularis thalami: a Golgi study. *Brain Res.* 1: 43–62, 1966.

SILVER, R. A., TRAYNELIS, S. F., AND CULL-CANDY, S. G. Rapid-time course of miniature and evoked excitatory currents at cerebella synapses in situ. *Nature* 355: 163–166, 1992.

SOLTESZ, I., SMETTERS, D. K., AND MODY, I. Tonic inhibition originates from synapses close to the soma. *Neuron* 14: 1273–1283, 1995.

SPREAFICO, R., DE CURTIS, M., FRASSONI, C., AND AVANZINI, G. Electrophysiological characteristics of morphologically identified reticular thalamic neurons from rat slices. *Neuroscience* 7: 629–638, 1988.

STERIADE, M. Thalamic origin of sleep spindles: Morison and Bassett (1945). *J. Neurophysiol.* 73: 921–922, 1995.

STERIADE, M., MCCORMICK, D. A., AND SEJNOWSKI, T. J. Thalamocortical oscillations in the sleeping and aroused brain. *Science* 262: 679–685, 1993.

TSENG, G.-F., PARADA, I., AND PRINCE, D. A. Double-labelling with rhodamine beads and biocytin: a technique for studying corticospinal and other projection neurons in vitro. *J. Neurosci. Methods* 37: 121–131, 1991.

ULRICH, D. AND HUGUENARD, J. R. $GABA_B$ receptor-mediated responses in GABAergic projection neurones of rat nucleus reticularis thalami in vitro. *J. Physiol. (Lond.)* 493: 845–854, 1996.

ULRICH, D. AND LUSCHER, H. R. Miniature excitatory synaptic currents corrected for dendritic cable properties reveal quantal size and variance. *J. Neurophysiol.* 69: 1769–1773, 1993.

VERDOORN, T. A., DRAGUHN, A., YMER, S., SEEBURG, P., AND SAKMANN, B. Functional properties of recombinant rat $GABA_A$ receptors depend on subunit composition. *Neuron* 4: 919–928, 1990.

VERDOORN, T. A. Formation of heteromeric γ-aminobutyric acid type A receptors containing two different alpha subunits. *Mol. Pharmacol.* 45: 475–480, 1994.

VON KROSIGK, M., BAL, T., AND MCCORMICK, D. A. Cellular mechanisms of a synchronized oscillation in the thalamus. *Science* 261: 361–364, 1993.

WATHEY, J. C., NASS, M. M., AND LESTER, H. A. Numerical reconstruction of the quantal event at nicotinic synapses. *Biophys. J.* 27: 145–164, 1979.

WEISS, D. S. AND MAGLEBY, K. L. Gating scheme for single GABA-activated Cl^- channels determined from stability plots, dwell-time distributions, and adjacent-interval durations. *J. Neurosci.* 9: 1314–1324, 1989.

WISDEN, W., LAURIE, D. J., MONYER, H., AND SEEBURG, P. H. The distribution of 13 $GABA_A$ receptor subunit mRNAs in the rat brain. I. Telencephalon, diencephalon, mesencephalon. *J. Neurosci.* 12: 1040–1062, 1992.

YEN, C. T., CONLEY, M., HENDRY, S. H., AND JONES, E. G. The morphology of physiologically identified GABAergic neurons in the somatic sensory part of the thalamic reticular nucleus in the cat. *J. Neurosci.* 5: 2254–2268, 1985.

ZHANG, S. J., HUGUENARD, J. R., AND PRINCE, D. A. Functional differences in $GABA_A$-mediated inhibition in nucleus reticularis thalami and somatosensory relay nuclei of the rat. *Soc. Neurosci. Abstr.* 20: 119, 1994.

ZHANG, S. J. AND JACKSON, M. B. GABA activated chloride channels in secretary nerve endings. *Science* 259: 531–534, 1993.

ZHANG, S. J. AND JACKSON, M. B. Neuroactive steroids modulate $GABA_A$ receptors in peptidergic nerve terminals. *J. Neuroendocrinol.* 6: 533–538, 1994.

ZHANG, S. J. AND JACKSON, M. B. Properties of $GABA_A$ receptor in rat posterior pituitary nerve terminals. *J. Neurophysiol.* 73: 1135–1144, 1995.